JOURNAL OF GUIDANCE, CONTROL, AND DYNAMICS
Vol. 17, No. 5, September–October 1994

New Results in Optimal Missile Avoidance Analysis

J. Shinar* and R. Tabak†
Technion—Israel Institute of Technology, Haifa 32000, Israel

Two-dimensional optimal avoidance of a proportionally guided coasting missile of first-order dynamics by a constant speed aircraft is analyzed. This model allows us to investigate the "missile outrunning" and "end-game evasion" maneuvers in the same engagement. Three regions of different optimal missile avoidance strategies are identified. All strategies are based on some compromise between the principles of "missile outrunning," bleeding energy from the missile and minimizing the closing velocity and the principles of optimal "end-game evasion," a final maneuver of a critical duration perpendicular to the line of sight. For any given initial geometry, the domain of initial ranges is divided into three zones: 1) a zone of short duration engagements, where the aircraft cannot fully implement either of the optimal evasion principles; 2) a zone wherein the principles of "end-game evasion" are satisfied and the dominant factor is missile dynamics; and 3) a zone wherein the missile drag is the major factor, and satisfaction of the "outrunning" principles is the essential feature. A synergetic interaction between aerodynamic drag and guidance dynamics increases the sensitivity of a missile guided by proportional navigation to evasive target maneuvers. Because of the missile aerodynamic drag, the aircraft can reduce missile maneuverability by an "outrunning" maneuver so that in the "end-game" a larger miss distance can be generated. The fresh insight gained by this investigation provides important cues for both aircraft and missile designers.

I. Introduction

THE avoidance of guided missiles is a very important factor for survivability in air combat. An avoidance maneuver is successful if it results in generating a miss distance that is larger than the "kill radius" of the missile warhead. If the type of missile, its guidance law, and other parameters are known, missile avoidance can be formulated as an optimal control problem of the aircraft willing to maximize the miss distance.

Although guided missiles are designed to have higher speed and maneuverability than the target aircraft, missile avoidance becomes feasible because of two phenomena. The kinetic energy of the missile, provided by a short duration propulsive phase, is rapidly dissipated by the aerodynamic drag. Consequently, the advantage of the missile over the aircraft (which preserves its energy) in speed and maneuverability is only temporary. The second element is the inherent dynamic delay of the guidance channel, which cannot cope with rapid changes of target acceleration in the terminal phase.

These phenomena lead us to consider missile avoidance in two stages. From long ranges, the aircraft can attempt to escape by maneuvering so that the missile is unable to reach its vicinity. This is known as a "missile outrunning" maneuver. If this maneuver is successful, aircraft survival is guaranteed. However, for shorter initial ranges the "outrunning" maneuver is not sufficient, and the aircraft has to maneuver near to the end of the engagement to take advantage of the delay in guidance dynamics. This is the "end-game evasion," a brief maneuvering sequence also known as the "last ditch maneuver."

In the known technical literature, the two stages of missile avoidance are analyzed separately using different mathematical models. Historically, end-game evasion studies,[1–6] all using constant speed missile models, were published first. Planar nonlinear kinematics were incorporated in Refs. 1 and 5, whereas in Refs. 2–4 and 6, a linearized kinematic model was used. Analysis of missile outrunning[7–11] is based on a variable speed missile model and nonlinear kinematics, while neglecting guidance dynamics for the sake of simplicity. In Ref. 12, an extensive simulation study with a rather complete missile model is presented. In all of these works, missiles guided by proportional navigation (PN) were considered.

Received July 10, 1992; revision received Aug. 20, 1993; accepted for publication Feb. 2, 1994.

*Professor, Faculty of Aerospace Engineering. Associate Fellow AIAA.
†Graduate Student.

The objective of this paper is to investigate both the missile outrunning and the end-game evasion in the same engagement. The simplest mathematical model for this purpose is that of a planar engagement between a constant speed aircraft and a coasting PN missile of first-order dynamics. With this model, the optimal control is a "bang-bang" type, and it can be computed by a simple search. The analysis presented in the paper is qualitative in nature, and the numerical results serve merely for illustrative purposes.

II. Problem Formulation

A. Mathematical Model

The mathematical model used in the investigation presented in this paper is based on the following assumptions:

1) The engagement is constrained to the horizontal plane, and the effect of gravity is neglected.
2) The missile and the aircraft both have perfect information.
3) Both the missile and aircraft are point masses.
4) Aircraft velocity is constant.
5) The aircraft responds instantaneously to commands.
6) Aircraft maneuverability is limited by the maximum turning rate.
7) The missile has no propulsion.
8) The missile has a parabolic drag polar with aerodynamic coefficients independent of Mach number.
9) The missile maneuverability is limited by the maximum lift coefficient.
10) The missile is guided by PN.
11) The missile guidance channel has a first-order transfer function.

The geometry of the engagement, depicted in Fig. 1, is described by the following set of differential equations:

$$\dot{R} = -V_M \cos(\psi - \chi_M) + V_T \cos(\psi - \chi_T) \triangleq f_R \qquad R(t_0) = R_0 \tag{1}$$

$$\dot{\psi} = 1/R[V_M \sin(\psi - \chi_M) - V_T \sin(\psi - \chi_T)] \triangleq f_\psi \qquad \psi(t_0) = \psi_0 \tag{2}$$

$$\dot{V}_M = -(1/m_M) D_M(V_M, L_M) \triangleq f_V; \quad V_M(t_0) = V_{M_0} \tag{3}$$

$$\dot{\chi}_M = (L_M/m_M V_M) = \Omega_M u_M; \quad \chi_M(t_0) = \chi_{M_0} \tag{4}$$

$$\dot{\chi}_T = (L_T/m_T V_T) = \Omega_T u_T; \quad \chi_T(t_0) = \chi_{T_0} \tag{5}$$

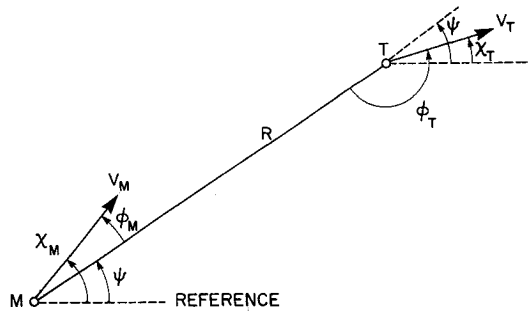

Fig. 1 Engagement geometry.

Equations (1) and (2) describe the relative motion between the missile and the target aircraft. The other three equations are of the respective point-mass dynamics, D and L are the aerodynamic drag and lift forces expressed in terms of the air density ρ, the appropriate reference surface S_i $(i = M, T)$, and the aerodynamic coefficients C_D and C_L:

$$L_i = (1/2)\rho(V^2 SC_L)_i \qquad i = M, T \tag{6}$$

$$D_M = (1/2)\rho(V^2 SC_D)_M \tag{7}$$

The missile drag coefficient is expressed by a parabolic model:

$$C_D = C_{D_0} + KC_L^2 \tag{8}$$

where C_{D_0} is the zero-lift drag coefficient, and K is the induced drag parameter. Moreover, $\Omega_i (i = M, T)$ are the maximum turning rates of the vehicles and $u_i (i = M, T)$ the respective normalized control variables satisfying $|u_i| \leq 1$.

By assumption 6, Ω_T is constant, whereas assumption 9 leads us to observe that

$$\Omega_M = \frac{1}{2}\frac{\rho S_M C_{L_{\max}}}{m_M} V_M = C_M V_M(t) \tag{9}$$

According to assumption 10, the turning rate command of the missile is controlled, as long as it doesn't reach saturation, by the PN guidance law[13]:

$$u_M = \frac{N' V_c}{V_M \Omega_M}\dot{\psi}_s = \frac{N' V_c(t)}{C_M V_M^2(t)}\dot{\psi}_s \tag{10}$$

where N' is the effective PN gain, $V_c = |f_R|$ is the closing velocity, and $\dot{\psi}_s$ is the line-of-sight rate both measured by the seeker. The relationship between $\dot{\psi}_s$ and the true line-of-sight rate $\dot{\psi} = f_\psi$ is represented by a first-order transfer function (see assumption 11) as given by the following:

$$\ddot{\psi}_s = 1/\tau[f_\psi - \dot{\psi}_s]; \quad \dot{\psi}_s(t_0) = 0 \tag{11}$$

The missile model described by (10) and (11) is shown in Fig. 2.

By expressing the equations of motion in a coordinate system attached to the line of sight, the state variables χ_M and χ_T are replaced by ϕ_M and ϕ_T (see Fig. 1), the system order is reduced, and the equations can be rewritten in a more compact form. Let us define the state vector $X \in R^5$ as follows:

$$\mathbf{X} = (R, V_M, \phi_M, \dot{\psi}_s, \phi_T)^T \tag{12}$$

and its dynamics by

$$\dot{X} = F(X, u_T); \quad X(t_0) = X_0 \tag{13}$$

The components of the right-hand side are the following:

$$F(X, u_T) = (f_R, f_V, f_M, f_S, f_T)^T \tag{14}$$

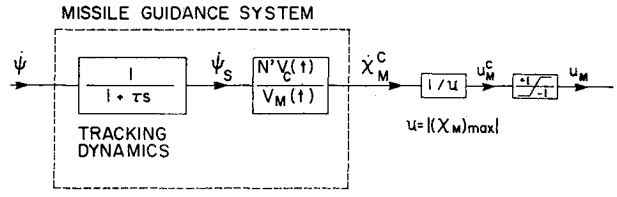

Fig. 2 Missile model.

with

$$f_R = -[V_T \cos\phi_T + V_M \cos\phi_M] \triangleq f_R(X) \tag{15}$$

$$f_V = -V_M^2[A_M + B_M u_M^2(X)] \triangleq f_V(X) \tag{16}$$

$$f_M = \Omega_M u_M(X) - f_\psi(X) \triangleq f_M(X) \tag{17}$$

$$f_S = 1/\tau[f_\psi(X) - \dot{\psi}_s] \triangleq f_S(X) \tag{18}$$

$$f_T = \Omega_T u_T - f_\psi(X) \triangleq f_T(X, u_T) \tag{19}$$

where

$$A_M = 1/2\rho(SC_{D_0}/m)_M \tag{20}$$

$$B_M = 1/2\rho(SKC_{L_{\max}}^2/m)_M \tag{21}$$

are given constants and

$$u_M(X) \triangleq \text{sat}\left\{\frac{N'|f_R(X)|}{C_M V_M^2}\dot{\psi}_s\right\} \tag{22}$$

$$f_\psi(X) \triangleq -[V_T \sin\phi_T + V_M \sin\phi_M]/R \tag{23}$$

are known functions of the state vector $\mathbf{X}$.

B. Optimal Control Problem

The optimal missile avoidance can now be formulated as an optimal control problem of the target aircraft.

Given a set of initial conditions

$$X_0 = (R_0, V_{M_0}, \phi_{M_0}, \dot{\psi}_{S_0}, \phi_{T_0}) \tag{24}$$

find the optimal control function $u_T^*(t)$, subject to

$$|u_T^*(t)| \leq 1 \tag{25}$$

that maximizes the "miss distance" (the distance of closest approach); i.e., minimizing

$$J = -R(t_f) \tag{26}$$

while satisfying the differential equations (13). The unspecified final time t_f is determined by a zero closing velocity (or the rather unlikely zero miss distance):

$$t_f \triangleq \arg\{R(t_f) \cdot f_R(t_f) = 0\} \tag{27}$$

This allows us to define an augmented terminal cost as

$$G(t_f) = -R(t_f) + \mu f_R(t_f) \tag{28}$$

where μ is a scalar multiplier to be found.

The variational Hamiltonian corresponding to this problem is the scalar product between $F(X, u_T)$ given in Eqs. (14–19) and the costate vector

$$\Lambda^T \triangleq (\lambda_R, \lambda_V, \lambda_M, \lambda_S, \lambda_T) \tag{29}$$

$$\mathcal{H} = \Lambda^T \cdot F(X, u_T) \tag{30}$$

Because the dynamic system (13) is autonomous, and the final time t_f is unspecified

$$\mathcal{H}^* \triangleq \mathcal{H}[u_T^*(t)] = \mathcal{H}^*(t_f) = 0 \tag{31}$$

The costate vector has to satisfy the adjoint differential equation,

$$\dot{\Lambda}^T = -\frac{\partial \mathcal{H}}{\partial X} \tag{32}$$

and the corresponding transversality conditions

$$\Lambda^T(t_f) = \left(\frac{\partial R}{\partial X} - \mu \frac{\partial f_R}{\partial X}\right)\Bigg|_{t_f} \tag{33}$$

Substituting Eq. (33) into Eqs. (30) and (31), yielding

$$\mathcal{H}^*(t_f) = f_R(t_f) - \mu\left[\frac{\partial f_R}{\partial X} \cdot F(X, u_T)\right]_{t_f} = 0 \tag{34}$$

leads us to determine (since the bracket does not vanish identically) that $\mu = 0$ and

$$\Lambda^T(t_f) = (1, 0, 0, 0, 0) \tag{35}$$

Application of the maximum principle provides the optimal control

$$u_T^* = \arg\max_{|u_T| \le 1} \mathcal{H} = \text{sign}\{\lambda_T\}; \quad \lambda_T \neq 0 \tag{36}$$

Because $\lambda_T(t_f) = 0$, the value of $u_T^*(t_f)$ is obtained by

$$u_T^*(t_f) = -\text{sign}\{\dot{\lambda}_T(t_f)\} = \text{sign}\left\{\frac{\partial \mathcal{H}}{\partial \phi_T}\right\}\Bigg|_{t_f} = \text{sign}\{V_T \sin \phi_T(t_f)\} \tag{37}$$

A singular optimal control requiring $\lambda_T(t) = \dot{\lambda}_T(t) = 0$ cannot be ruled out. A detailed analysis[14] shows, however, that it mainly occurs near the end of an engagement when the missile is saturated ($|u_m| = 1$) and is of a very short duration. Thus, it has no significant effect on the miss distance.

III. Solution Methodology

The solution of the high-dimensional nonlinear two-point boundary value problem defined by 10 differential equations (13) and (32) with the associated boundary conditions (24) and (35) requires a substantial computational effort. Fortunately, the bang-bang structure of the optimal control in Eq. (36) allows a rather simple way to solve the problem.

The numerical results were obtained by the following method. Engineering intuition (confirmed by some experience) suggested that for short initial ranges the evading aircraft does not change the direction of the evasive maneuver. Therefore, for a given initial geometry (ϕ_{M_0}, ϕ_{T_0}), we can start at a short range and find, by forward integration of the equations of motion (13), the direction of the optimal evasive maneuver (left or right) by direct comparison. Increasing the initial range, one can identify the existence of an eventual direction change of the maneuver by a one-dimensional search. Once the time of the maneuver change (switch) which maximizes the miss distance is found, its optimality is verified by backward integration of the costate equations (32) along the trajectory and by comparing the best switching time obtained by the search with the occurrence of $\lambda_T = 0$. This iterative verification process provides a fine adjustment of the optimal switch time and the resulting miss distance.

For any new initial range $(R_0)_{\text{new}} = (R_0)_{\text{old}} + \Delta R_0$, the optimal solution of the previous step serves as the first guess. The step by step increase of R_0 is stopped when the optimal miss distance exceeds a sufficiently large prescribed value (e.g., $R(t_f) \ge 50$ m). At this point the entire computational process restarts with a new initial geometry at a short range.

In order not to exceed the computational resources a well defined subspace of admissible initial conditions was selected. Two of the five components of the initial state X_0 in (24) were taken as constants. In addition to $\psi_s(t_0) = 0$, stated in (11), the value of $V_{M_0} = 800$ m/s was kept unchanged in all examples. Moreover, the value of ϕ_{M_0} was determined by a zero value of the initial line of sight rate (i.e., a "collision course") which yields, based on (2),

$$\phi_{M_0} = \sin^{-1}\{-V_T \sin \phi_{T_0} / V_{M_0}\} \tag{38}$$

Selecting "collision course" initial conditions is based on the assumption that the missile succeeds to correct the eventual launching errors before the beginning of the coasting phase, modelled in this study.

These restrictions allowed a systematic scanning of the (R, ϕ_M, ϕ_T) subspace using two independent initial conditions R_0 and ϕ_{T_0} (by symmetry $0 \le \phi_{T_0} \le \pi$). The numerical solution process has been very efficient and resulted in good precision with moderate computational effort.

All computations were based on the set of engagement parameters summarized in Table 1.

The results obtained by the computation process for an effective PN gain of $N' = 3.2$ are presented and discussed in the next section. Additional results can be found in Ref. 14.

Table 1 Engagement data

Engagement altitude	$h = 6$ km
Target velocity	$V_T = 300$ m/s
Target turning rate	$\Omega_T = 0.16$ rad/s
Initial missile velocity	$V_{M_0} = 800$ m/s
Missile time constant	$\tau = 0.5$ s
Missile mass	$m_M = 100$ kg
Missile reference surface	$S_M = 0.025$ m^2
Missile aerodynamic coefficients	$(C_L)_{\max} = 8.0$
	$C_{D_0} = 0.7$
	$K = 0.05$

IV. General Qualitative Discussion

The optimal missile avoidance maneuver found in the present investigation consists of two major elements: an initial turn and an eventual "last ditch" maneuver. For $N' = 3.2$, the maximum number of changes in the maneuver direction (switches) doesn't exceed two. To understand the nature of this missile avoidance maneuver, it is necessary to repeat briefly the "principles of optimal evasion" found in previous works.

The principles of "missile outrunning" were established in Refs. 8 and 9 assuming a coasting PN missile with ideal guidance dynamics. According to this study, the first principle (P-O1) requires the aircraft to turn in a direction that minimizes the closing velocity of the missile. The second principle (P-O2) states that continuous maneuvering bleeds energy from the missile by taking advantage of the PN guidance law. This phenomenon develops in the following sequence: 1) target maneuvering ($u_T \neq 0$) generates a line-of-sight rotation, as expressed by f_ψ in Eq. (23); 2) the PN guidance law requires missile turning rate u_M proportional to f_ψ; and 3) the induced drag of the missile is proportional to u_M^2, Eq. (16). Because f_ψ is inversely proportional to R, the effect becomes stronger as the missile approaches the target. This phenomenon is clearly illustrated in Fig. 3, where velocity profiles of the missile are depicted for a minimum closing velocity ("tail chase") initial conditions against a nonmaneuvering target (dashed line), and against the optimal target maneuver (solid line). The energy loss of the missile induced by the maneuver also leads to a longer "time of capture."

The principles of optimal "end-game evasion" were first determined using a linearized kinematic model, based on the assumption of constant missile velocity.[3] The essential element of the maneuver is a last-ditch direction change of the target acceleration, perpendicular to the line-of-sight. The time-to-go of this switch is proportional to the missile time constant τ for any given set of parameters. Taking into account the nonlinear kinematic effects in such a maneuver, two principles of the optimal evasion were formulated in Ref. 9 for a set of fixed parameters: (P-E1) the last maneuver is of constant duration, proportional to the missile time constant; (P-E2) the initial turn has to position the target in a direction that enables the last maneuver to be performed perpendicular to the line-of-sight. Both principles can be fully satisfied only if the initial range is sufficiently

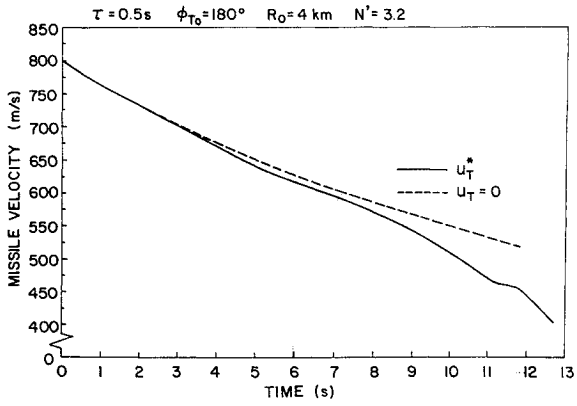

Fig. 3 Missile velocity profiles (tail chase).

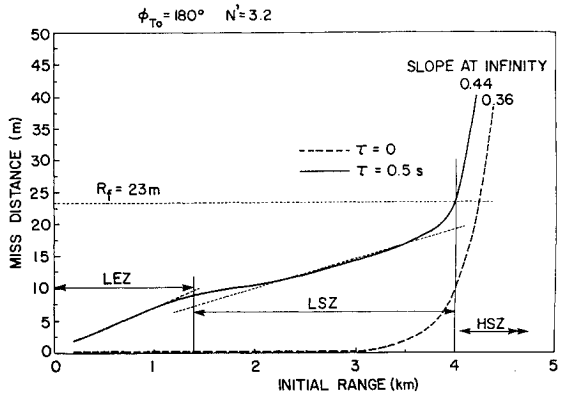

Fig. 4 Optimal miss distance vs initial range (tail chase).

large. For shorter ranges, an optimal compromise has to be reached, resulting in a reduced miss distance.

The end-game evasion exploits the dynamic delay of the missile guidance system (modeled by the time constant τ), as can be seen in Fig. 4, which shows that in this example for initial ranges of less than 3 km, the miss distance of an "ideal" missile ($\tau = 0$) is zero. (For larger ranges the missile outrunning starts to take effect.)

This figure also illustrates that, for a given initial geometry, the domain of the initial ranges can be divided into three zones:

1) There is a "low effectiveness zone" (LEZ) of short ranges where the principles of end-game evasion cannot be fully satisfied in a planar engagement. Therefore, in this zone, the optimal miss distances are rather small and increase with the initial range.

2) The second zone is called the "low sensitivity zone" (LSZ). Here the optimal miss distance is a *slowly* increasing function of the initial range.

3) For longer ranges (beyond 4 km in this example), the optimal miss distance exhibits a very high sensitivity to variations of the initial range. This "high sensitivity zone" (HSZ) is dominated by the effects of missile outrunning, i.e., the effects of aerodynamic drag embedded in the variable speed missile model.

It is in the low sensitivity zone that the aerodynamic drag and the guidance dynamics interact in affecting the optimal missile avoidance, as is elaborated in the next section.

V. Analysis of the Low Sensitivity Zone

The effect of guidance dynamics for a constant velocity missile model ($V_M > V_T$) were stated in Ref. 9 in a nondimensional form. The normalized miss distance M^* is

$$M^*[R(t_f)/a_T\tau^2] = f_1(N', \mu, \theta_f, \Gamma) \tag{39}$$

where a_T is the maximal lateral target acceleration

$$a_T = \Omega_T V_T \tag{40}$$

μ is the missile/target acceleration ratio

$$\mu \triangleq \left(\frac{\Omega_M V_M}{\Omega_T V_T}\right) \tag{41}$$

θ_f is the normalized duration of the engagement

$$\theta_f = (t_f/\tau) \tag{42}$$

and Γ is a dynamic similarity parameter defined by

$$\Gamma \triangleq \Omega_T \tau \tag{43}$$

which has to be sufficiently small for the validity of a linearized analysis.

The normalized time-to-go of the last ditch maneuver change θ_s is

$$\theta_s \triangleq (t_f - t_s/\tau) = f_2(N', \mu, \theta_f, \Gamma) \tag{44}$$

Both f_1 and f_2 decrease monotonically with increasing μ.

For a constant speed missile model, μ remains constant. However, for the present variable speed model, substituting Eqs. (9) and (40) into Eq. (41) results in

$$\mu = (C_M/a_T)V_M^2(t) \tag{45}$$

which indicates a monotonical decrease as the initial range increases.

The missile velocity profile, plotted in Fig. 5 as a function of the initial range, indicates the monotonically decreasing nature of this relationship and the effect induced by optimal target maneuvering. We can conclude, therefore, that initial target maneuvering in the missile outrunning phase leads to a less maneuverable missile in the end game. Consequently, the optimal miss distance increases with initial range.

In Figs. 6 and 7, a comparison between the present work and of the linearized analysis of Ref. 3 is presented. In the linearized model, different constant speed missiles were used, and all engagements had the same duration of 10 time constants. The variable speed coasting missile used in the present study begins its flight at different initial ranges, resulting in different engagement times and different final velocities. To represent the average maneuverability of the missile in the end-game (for the sake of comparison), the value of the velocity at the last switch was selected as the characteristical one.

The comparison shows a reasonably good correspondence of the results, despite the differences in the models. If the engagement duration is $5 \leq \theta_f \leq 20$, there is an almost perfect matching. The difference for high velocities; i.e., short initial ranges ($\theta_f < 5$), is explained by the fact that these engagements start in the low effectiveness zone. These results are compatible with Fig. 4 and Ref. 9. For engagements starting at long ranges ($\theta_f > 20$) and leading to a low characteristic velocity, the nominal zone (the last 10 time constants of the engagement) starts with a nonzero line-of-sight rate caused by the initial outrunning maneuver. This induces a slight change in the time of the last switch and an increase in the optimal miss distance.

It can be summarized that the interaction between the initial outrunning maneuver (exploiting the aerodynamic drag of the missile and its PN guidance law) and the "end-game evasion" (which takes advantage of the delay of the guidance dynamics) is clearly synergetic. The missile outrunning maneuver, although it cannot fully

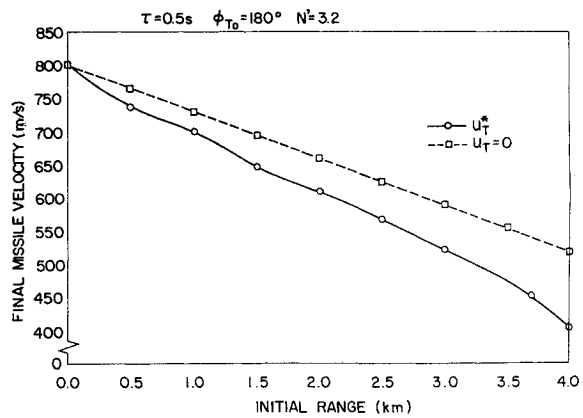

Fig. 5 Final missile velocity vs initial range (tail chase).

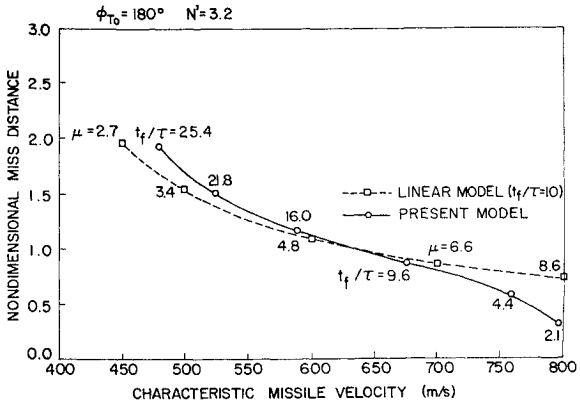

Fig. 6 Miss distance comparison with linear models (tail chase).

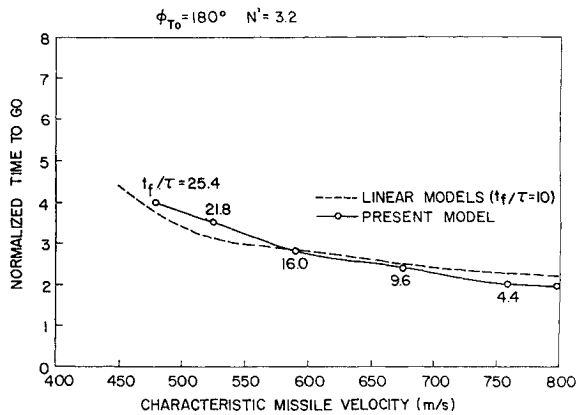

Fig. 7 "Last switch" comparison with linear models (tail chase).

accomplish its original objective to deny the missile reaching the target vicinity, provides the most favorable conditions for the last ditch maneuver.

VI. Optimal Avoidance Strategies

One of the tasks in the present investigation has been to identify the nature of optimal missile avoidance strategies against a variable speed PN missile with first-order guidance dynamics. The results allow us to decompose the subspace of initial conditions of interest into three regions of different optimal missile avoidance strategies, as shown in Fig. 8.

The region D_1, where strategy S1 is optimal, is confined to the forward sector ($0 \leq \phi_{T_0} \leq 90$ deg) and characterized by the fact that the aircraft does not have sufficient time to turn toward the minimum closing velocity (tail-chase) direction. For this reason, the first principle of missile outrunning (P-O1) cannot be satisfied. Thus, S1 can be considered as an optimal compromise in satisfying the remaining three principles of optimal evasion: (P-O2), (P-E1), and (P-E2). The optimal trajectories in this region tend toward a head-on geometry ($\phi_T \approx 0$) so that the last-ditch maneuver can be performed nearly perpendicular to the line of sight. It is shown in Fig. 9 that for shorter ranges, the aircraft starts to turn toward the missile in order to be able to satisfy (P-E2), while for longer ranges, the initial turn is away from the missile in order to increase the line-of-sight rate (P-O2), and the direction of the turn is changed at the best time for satisfying both end-game principles (P-E1, P-E2). It should be noted that the region D_1 depends very strongly on the aircraft maximum turning rate Ω_T. The higher Ω_T is, the smaller is D_1.

The region D_2 is a union of that part of the forward sector, where a turn toward "tail-chase" ($\phi_T = 180$ deg) can be completed, and a large portion of the rear sector (90 deg $\leq \phi_{T_0} \leq$ 180 deg). In D_2, all four principles of missile avoidance take part in the optimal compromise designated by the strategy S2. All optimal trajectories in D_2 tend toward a tail-chase geometry, where the last-ditch maneuver is performed. The direction of the initial turn depends on the initial conditions, as shown in Fig. 9.

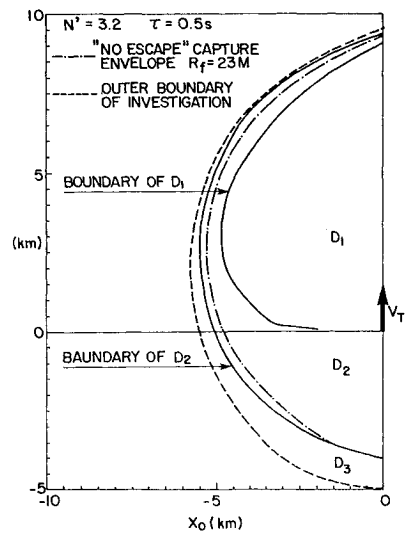

Fig. 8 Initial state space partition.

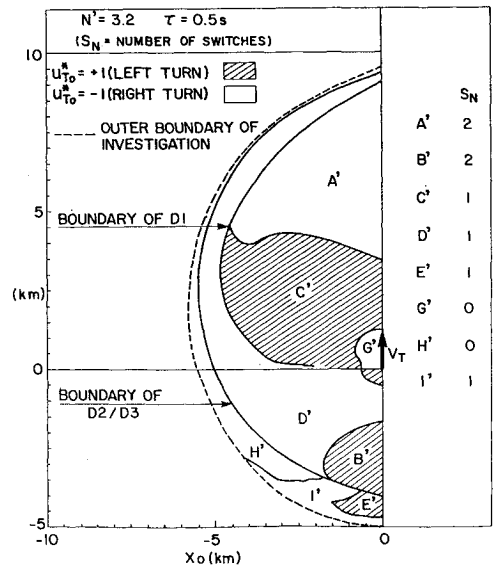

Fig. 9 Optimal switching envelopes.

The region D_3 is a "ring" of rather long initial ranges in the entire domain ($0 \leq \phi_{T_0} \leq 180$ deg). The corresponding strategy S3 is based on the satisfaction of the missile outrunning principles (P-O1) and (P-O2). Optimal trajectories in D_3 all terminate in a tail-chase with a low final velocity and a large miss distance, $R(t_f) \geq 23$ m. D_3 is contained entirely in the high sensitivity zone. In most cases, the final maneuver is insignificant, and frequently it disappears totally.

From the point of view of onboard implication, the results of this study indicate the need for early detection of guided missiles in order to allow a successful avoidance maneuver. Reliable measurements of the relative state and good intelligence about the missile parameters (which may require also real-time threat identification) are necessary requirements for computing the optimal missile avoidance maneuver. Because in this work the structure of the optimal missile avoidance strategies has been identified, the solution for any guided missile can be precomputed, parametrized, and stored. Based on these data, once the missile is detected and the relative state is measured, the actual avoidance parameters; i.e., the direction of the initial turn and the timing of the direction changes; are easily determined.

VII. Conclusions

The present paper is the first one in the open literature where the two stages of the optimal missile avoidance, namely the missile outrunning and the last ditch end-game evasion, are investigated in

the same engagement. The use of the simplest mathematical model suitable for such an investigation allowed us to concentrate on the main features and also to obtain a numerical solution with moderate computational effort. The main contribution of this analysis is the discovery of the synergetic interaction between the aerodynamic drag and the dynamic lag of the guidance channel, which is the reason that a PN guided missile is more sensitive to avoidance maneuvers than it was assumed in the past. Currently operational PN guided missiles can be avoided, because their designers failed to take into account optimal missile avoidance maneuvers. The need for an improved guidance law in future missile designs is obvious.

References

[1]Julich, P. M., and Borg, A. D., "Proportional Navigation vs. an Optimally Evading Constant Speed Target in Two Dimensions," *Journal of Spacecraft and Rockets*, Vol. 7, No. 12, 1970, pp. 1454–1457.

[2]Slater, G. L., and Wells, W. R., "Optimal Evasive Tactics Against a P.N. Missile with Time Delay," *Journal of Spacecraft and Rockets*, Vol. 10, No. 5, 1973, pp. 309–313.

[3]Shinar, J., and Steinberg, D., "Analysis of Optimal Evasive Maneuvres Based on a Linearized Two-Dimensional Kinematic Model," *Journal of Aircraft*, Vol. 14, No. 8, 1977, pp. 795–802.

[4]Shinar, J., Rotsztein, Y., and Bezner, E., "Analysis of Three-Dimensional Optimal Evasion with Linearised Kinematics," *Journal of Guidance and Control*, Vol. 2, No. 5, 1979, pp. 353–360.

[5]Forte, I., Steinberg, A., and Shinar, J., "The Effects of Non-Linear Kinematics in Optimal Evasion," *Optimal Control Applications and Methods*, Vol. 4, No. 2, 1983, pp. 139–152.

[6]Ben-Asher, J. Z., and Cliff, E. M., "Optimal Evasion Against a Proportionally Guided Pursuer," *Journal of Guidance, Control, and Dynamics*, Vol. 12, No. 4, 1989, pp. 598–600.

[7]Shinar, J., "Missile Avoidance Maneuvers of Longer Duration," TAE Report No. 564, Faculty of Aerospace Engineering, Technion, Haifa, Israel, Jan. 1985.

[8]Shinar, J., "State-dependant Optimality of a Singular Subarc," *Automatica*, Vol. 24, No. 2, 1988, pp. 195–201.

[9]Silberman, G., and Shinar, J., "On Capture Zone of Coasting Missiles Guided by Proportional Navigation," *Proceedings of the 30th Israel Annual Conference on Aviation and Astronautics*, 1989.

[10]Shinar, J., Guelman, M., Silberman, G., and Green, A., "On Optimal Missile Avoidance—A Comparison Between Optimal Control and Differential Game Solutions," *Proceedings of the 1989 IEEE International Conference on Control and Applications*, Inst. of Electrical and Electronics Engineers, Jerusalem, 1989.

[11]Silberman, G., "Optimal Evasion of a Constant Speed Target from a Proportional Navigation Coasting Missile," M.S. Thesis, Faculty of Aerospace Engineering, Technion, Haifa, Israel, Sept. 1989 (in Hebrew).

[12]Imado, F., and Miwa, S., "Fighter Evasive Maneuvres Against Proportional Navigation Missile," *Journal of Aircraft*, Vol. 23, No. 11, 1986, pp. 825–830.

[13]Murtaugh, S., and Criel, H., "Fundamentals of Proportional Navigation," *IEEE Spectrum*, Vol. 3, No. 12, 1966, pp. 75–85.

[14]Tabak, R., "Optimal Evasion of an Aircraft from a Coasting Proportional Navigation Guided Missile," M.S. Thesis, Faculty of Aerospace Engineering, Haifa, Israel, Technion, Aug. 1991.